

Variations and climatology of ClO in the polar lower stratosphere from UARS Microwave Limb Sounder measurements

M. L. Santee

Jet Propulsion Laboratory, California Institute of Technology, Pasadena, California, USA

G. L. Manney

Jet Propulsion Laboratory, California Institute of Technology, Pasadena, California, USA

Department of Natural Sciences, New Mexico Highlands University, Las Vegas, New Mexico, USA

J. W. Waters and N. J. Livesey

Jet Propulsion Laboratory, California Institute of Technology, Pasadena, California, USA

Received 19 December 2002; revised 26 March 2003; accepted 4 April 2003; published 7 August 2003.

[1] The Microwave Limb Sounder (MLS) on board the Upper Atmosphere Research Satellite (UARS) measured the global distribution of stratospheric ClO over annual cycles for much of the 1990s, albeit with reduced sampling frequency in the latter half of the decade. Here we present an overview of the interannual and interhemispheric variations in the distribution of ClO derived from UARS MLS measurements, with a particular emphasis on enhancements in the winter polar lower stratosphere. Although ClO enhancement within the Arctic vortex is comparable in both magnitude and spatial extent to that in the Antarctic at 465 K (~19 km), a significant interhemispheric disparity is seen at higher altitudes, where maximum ClO abundances, and their spatial extent, are considerably larger in the Antarctic than in the Arctic. The Arctic exhibits much more interannual variability in the magnitude, timing, and distribution of ClO enhancement than does the Antarctic. Nevertheless, during the mid-1990s, when the Arctic lower stratosphere was atypically cold, MLS observed the Arctic vortex to be almost completely filled with enhanced ClO in midwinter to late winter. The peak in the ClO profile is at a higher altitude, and the vertical extent of chlorine activation is larger, in the Antarctic than in the Arctic. The Arctic winter of 1995/1996, however, stands out as having a much more Antarctic-like ClO distribution, with larger maximum ClO abundances, a higher altitude for the profile peak, and greater horizontal and vertical extent of activation than the other winters observed by UARS MLS. In the Southern Hemisphere, ClO becomes enhanced in the sunlit portions of the vortex by at least late May/early June every year, whereas in the Northern Hemisphere, ClO becomes enhanced in mid to late December in some years but not until January in others. Elevated levels of reactive chlorine persist for 4–5 months in the south but only 2–3 months in the north.

INDEX TERMS: 0340 Atmospheric Composition and Structure: Middle atmosphere—composition and chemistry; 0341 Atmospheric Composition and Structure: Middle atmosphere—constituent transport and chemistry (3334); 0394 Atmospheric Composition and Structure: Instruments and techniques; **KEYWORDS:** Microwave Limb Sounder (MLS), Upper Atmosphere Research Satellite (UARS), chlorine activation, chlorine monoxide (ClO), stratospheric chemistry, polar processing

Citation: Santee, M. L., G. L. Manney, J. W. Waters, and N. J. Livesey, Variations and climatology of ClO in the polar lower stratosphere from UARS Microwave Limb Sounder measurements, *J. Geophys. Res.*, 108(D15), 4454, doi:10.1029/2002JD003335, 2003.

1. Introduction

[2] Chemical ozone loss at high latitudes in the stratosphere is directly controlled by the extent and temporal evolution of active chlorine [e.g., Solomon, 1999; World

Meteorological Organization, 1999]. In turn, the magnitude, spatial extent, and duration of chlorine activation in the lower stratosphere are controlled by meteorological conditions, in particular the variability, permeability, areal extent, distortion and elongation, and persistence of the winter polar vortex and the frequency of occurrence, location, and persistence of low temperatures (which govern the formation of polar stratospheric clouds, PSCs). The Northern and

Southern Hemispheres are characterized by distinctly different seasonal temperature patterns and vortex behavior. Lower stratospheric winter temperatures are $\sim 15\text{--}20$ K higher, on average, and the vortex is smaller, weaker, more distorted, more variable, and shorter-lived in the Arctic than in the Antarctic [e.g., *Andrews*, 1989; *Waugh and Randel*, 1999; *Waugh et al.*, 1999]. Whereas in the south temperatures in the lower stratospheric vortex tend to exhibit a more or less steady decline beginning in fall to (and below) the thresholds for PSC formation, in the north greater dynamical activity is accompanied by rapid temperature variations. In general these conditions lead to fewer, less persistent PSC events in the Arctic [e.g., *Poole and Pitts*, 1994; *Fromm et al.*, 1999]. During the mid-1990s, however, the Arctic lower stratospheric vortex was unusually strong and long-lived [*Waugh et al.*, 1999], less variable from year to year, and atypically cold, with prolonged periods of temperatures low enough for extensive PSC formation [e.g., *Zurek et al.*, 1996; *Pawson and Naujokat*, 1999]. Although somewhat extreme in the context of the climatological record, the conditions of the mid-1990s may be representative of more typical meteorological situations in the future, if the lower stratosphere cools in the coming decades in response to climate change [e.g., *World Meteorological Organization*, 2003, and references therein].

[3] Launched in September 1991, the Microwave Limb Sounder (MLS) on board the Upper Atmosphere Research Satellite (UARS) measured the global distribution of stratospheric CIO for a decade, although its measurement sampling became much more irregular in later years. The majority of the MLS measurements were obtained during the unusually cold conditions of the mid-1990s. Although MLS CIO data have been presented previously for one southern [*Waters et al.*, 1993a, 1993b; *Santee et al.*, 1995] and most northern [*Waters et al.*, 1993b, 1995; *Manney et al.*, 1994b, 1996a; *Santee et al.*, 1996a, 1997, 2000] winters during the MLS lifetime, and have been used in investigations of the chlorine deactivation process [*Douglass et al.*, 1995; *Santee et al.*, 1996b], until now no overall synthesis of what has been learned from the data collected in individual winters has been carried out. Furthermore, the previous studies focused mainly on a single level (465 K) in the lower stratosphere. Finally, all of the previous studies examined either version 3 or version 4 MLS data. Changes in the MLS CIO profiles in version 5 (the definitive MLS data version) warrant a thorough evaluation of the entire reprocessed data set. We undertake such an assessment here, with a view toward establishing an overall picture of the behavior of enhanced CIO in both hemispheres in the 1990s.

[4] This paper focuses on the lower stratosphere, from 420 to about 700 K in potential temperature ($\sim 17\text{--}28$ km altitude). UARS MLS also measured CIO in the upper stratosphere, where the distribution of reactive chlorine is controlled not by winter polar processes but rather primarily by the distribution of CH_4 ; the diurnal and seasonal variations and the trends over the 1991–1997 time period in MLS CIO in this region were investigated by *Ricaud et al.* [2000] and *Froidevaux et al.* [2000], respectively. The possible activation of chlorine in cirrus clouds or PSCs in the tropopause region and lowermost stratosphere (below ~ 380 K, ~ 15 km) has also been a topic of recent interest

[e.g., *Borrmann et al.*, 1996, 1997; *Solomon et al.*, 1997; *Lelieveld et al.*, 1999; *Smith et al.*, 2001; *Lee et al.*, 2002]. We cannot address this issue, however, as UARS MLS CIO data are not available at these altitudes. This paper concentrates on the seasonal enhancements in CIO at high latitudes. At low latitudes and midlatitudes under nonperturbed conditions, lower stratospheric CIO abundances are typically less than ~ 0.05 ppbv [*Toohey et al.*, 1991, 1993; *Avallone et al.*, 1993]. UARS MLS CIO measurements lack sufficient precision to reliably track day-to-day changes in abundances of this magnitude (even in zonal means). However, CIO mixing ratios at low latitudes and midlatitudes can be substantially enhanced under volcanic conditions [*Avallone et al.*, 1993; *Toohey et al.*, 1993; *Dessler et al.*, 1993]. *Froidevaux et al.* [2000] examined trends in lower stratospheric CIO using MLS data and found that CIO abundances diminished by a factor of 2–4 at low latitudes and midlatitudes over the period 1992 to 1997, consistent with a relaxation to nonenhanced conditions after the eruption of Mt. Pinatubo; the issue of volcanically enhanced CIO at lower latitudes will not be considered further here.

[5] In section 2 we briefly review the UARS MLS instrument and data coverage and summarize the quality of the version 5 CIO measurements. In section 3 we present daily maps and equivalent latitude/potential temperature (EqL/ θ) cross sections to show interhemispheric and interannual differences in wintertime CIO abundances. Then in section 4 we examine time series of different slices through the data to develop a comprehensive picture of the mean evolution of enhanced CIO in the winter polar vortices of both hemispheres. Section 5 summarizes the main conclusions.

2. Measurement Description

2.1. MLS Data Coverage

[6] Microwave limb sounding in general and the UARS MLS instrument in particular are described in detail by *Waters* [1993] and *Barath et al.* [1993], respectively. Briefly, MLS measured stratospheric emission from the CIO rotational transition at 204.352 GHz (1.47 mm) using a heterodyne technique. A calendar of MLS daily data coverage is presented by *Livesey et al.* [2003]. After several years in orbit, degradation in the performance of the MLS antenna scan mechanism, together with a reduction in power available from the UARS spacecraft, resulted in markedly reduced data sampling. Measurement frequency continued to decline until the instrument was placed in standby mode in July 1999. Although MLS was turned on for two brief intervals during the extremely cold Arctic winter of 1999/2000 [*Santee et al.*, 2000] and again in August 2001, the relative sparsity of the data collected after 1998 limits their utility in establishing a climatology of this kind, and they are not included here.

[7] Latitudinal coverage of the MLS measurements extended from 80° on one side of the equator to 34° on the other. The UARS orbit plane precessed in such a way that all local solar times were sampled in ~ 36 days (a “UARS month”), getting ~ 20 min earlier each day at a given latitude. The orbital geometry led to the occurrence of a brief interval in the middle of every UARS month when MLS made measurements only in darkness. This period of

nighttime-only observations has important implications for species such as ClO that exhibit strong diurnal cycles and will be discussed further in subsequent sections. To keep MLS (and other instruments) on the shaded side of the spacecraft, a 180° yaw maneuver was performed at the end of every UARS month. Thus 10 times per year MLS alternated between viewing northern and southern high latitudes, with the first day of a particular UARS month occurring ~5 days earlier each year. As a consequence, on a particular day of the year MLS may have been viewing northern high latitudes in some years but southern high latitudes in other years. Another consequence of this interruption in high-latitude coverage, combined with the increasing paucity of the data toward the end of the mission, is that the complete period of chlorine deactivation in the Southern Hemisphere was never captured in the MLS data.

2.2. MLS ClO Data Quality

[8] A full description of the MLS version 5 (v5) retrieval algorithms and resulting data set is given by *Livesey et al.* [2003], including comparisons with previous ClO data versions; *Livesey et al.* [2003] update the validation of version 3 MLS ClO measurements given by *Waters et al.* [1996]. Here we very briefly describe the major changes in the algorithms and their impact on the ClO retrievals.

[9] In v5 geophysical parameters are retrieved on every UARS surface (six surfaces per decade change in pressure, as opposed to three in previous MLS data sets). The v5 retrievals thus allow better definition of the ClO profile. The inherent vertical resolution of the instrument is coarser than the v5 retrieval grid, however, so vertical smoothing is applied to the retrieval system to more closely reflect the instrument resolution and enhance retrieval stability. As a consequence, the true vertical resolution of the v5 ClO data (4–5 km) is approximately the same as, and the v5 profiles are generally smoother than, the previous versions. During periods of strong ClO enhancement (e.g., August/September in the Antarctic, January/February in the Arctic), the peak in the ClO profile has typically moved up from 46 hPa in v4 to 32 hPa (not formerly a retrieval surface) in v5. In addition, at 100 hPa the v5 data are more stable and have more realistic values than in previous versions. Estimated precision and accuracy for the v5 ClO data are the same as or slightly better than those for v4 (depending on the level). For the levels of interest here (100–10 hPa), the typical single-profile precision (1σ) is 0.3–0.4 ppbv (except at 100 hPa, where it is 0.6 ppbv), and the estimated accuracy (at the ~90–95% confidence level, roughly 2σ) is 15% (scaling uncertainty) plus a bias uncertainty of 0.15 ppbv in the winter polar vortices (0.2 ppbv at 100 hPa). To conserve spacecraft power, after 15 June 1997 MLS was operated without the 63-GHz radiometer, necessitating a change in the v5 data processing algorithms [*Livesey et al.*, 2003]. Differences of up to ~0.2 ppbv at 100 hPa and under polar enhanced conditions, and up to ~0.05 ppbv elsewhere, are seen between the data collected before and after June 1997 [*Livesey et al.*, 2003].

[10] In v5 CH₃CN is retrieved instead of SO₂; this allows a better fit of the measured radiances when there is a negligible amount of volcanically injected SO₂ in the stratosphere, including a fit of some residual curvature in the spectra that previously led to unrealistic negative values

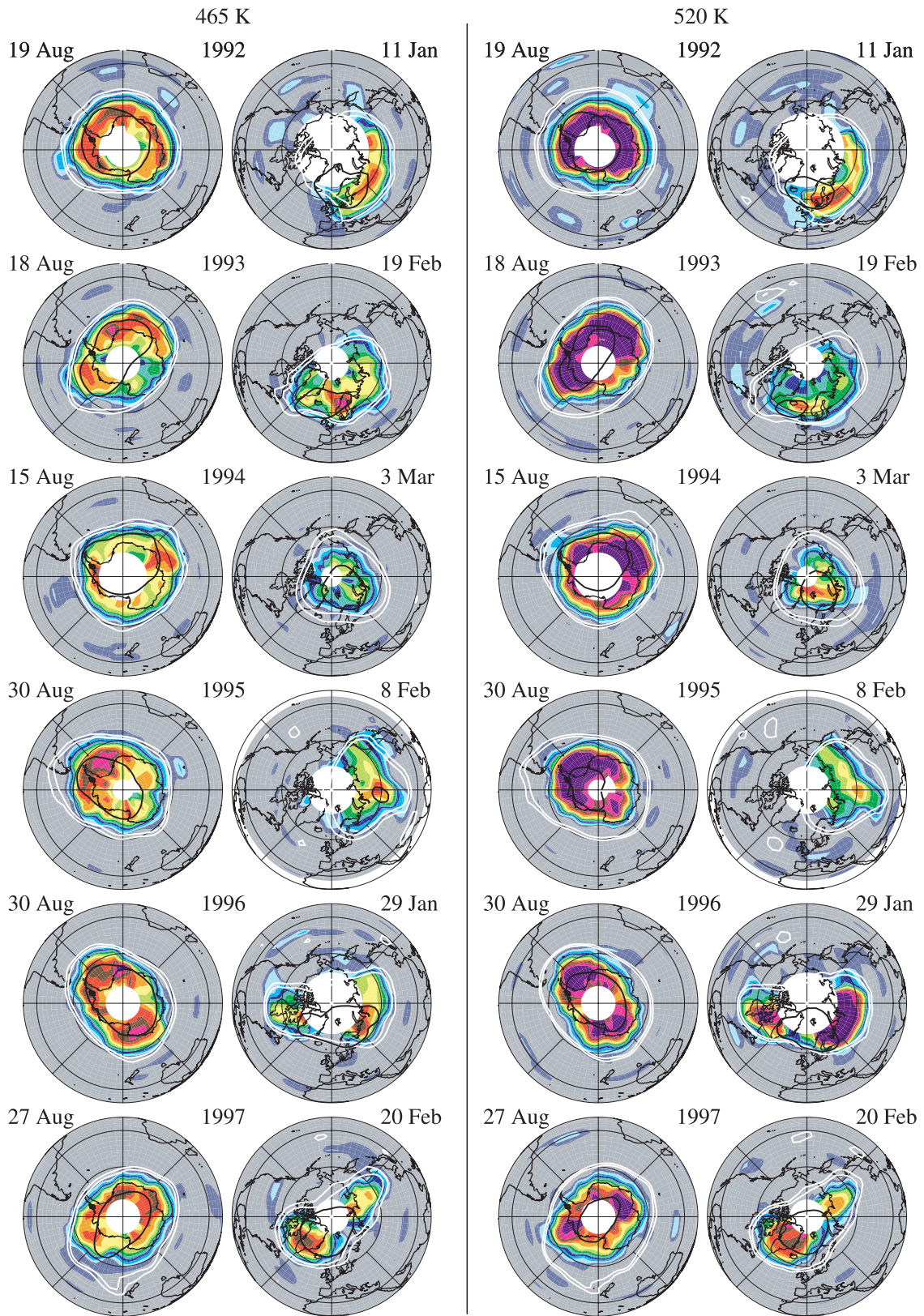
in averaged nighttime ClO between ~22 and ~4.6 hPa. As in earlier data versions, however, nonlinearities with respect to temperature in the MLS retrieval system can cause retrieved ClO values to be up to approximately 5–10% too large in the cold winter polar (especially Antarctic) vortex. This effect has not been thoroughly quantified, but it is believed to be covered by the stated uncertainties.

3. Daily Snapshots of ClO Behavior

[11] To compare the wintertime enhancement of ClO in both polar regions from year to year, we present in Figure 1 maps of daytime MLS ClO interpolated to two potential temperature surfaces in the lower stratosphere: 465 K (corresponding to ~19 km) and 520 K (corresponding to ~22 km). Here “daytime” data are defined to be those for which the local solar zenith angle (SZA) is less than 88°. The days shown were selected to represent the period of maximum observed ClO enhancement each winter, constrained by the UARS yaw cycles, other data gaps, and local SZA conditions. Of course, it should be noted that some of the variability displayed in these plots arises from day-to-day, rather than interannual, variations.

[12] At 465 K ClO enhancement within the Arctic vortex is fairly comparable in both magnitude and spatial extent to that in the Antarctic. *Brune et al.* [1990] were the first to note, on the basis of in situ measurements made from the ER-2 aircraft, that ClO mixing ratios inside the perturbed Arctic vortex can be as large as those in the Antarctic. Similar findings were obtained through comparison of ground-based millimeter-wave ClO measurements taken at McMurdo and Ny Ålesund [*Nagar et al.*, 1999]. UARS MLS provided the first hemispheric maps of ClO; in reporting early results from MLS, *Waters et al.* [1993b] showed that in both hemispheres the winter polar vortex becomes almost completely filled with enhanced ClO, with abundances large enough to indicate virtually complete conversion of stratospheric chlorine to reactive forms. However, all of these studies, and subsequent studies using MLS ClO data, focused on approximately the 20-km, or 465-K, level. As seen in Figure 1, a much greater interhemispheric disparity occurs at 520 K, where maximum abundances, and their spatial coverage, are considerably larger in the Antarctic than in the Arctic in most years. A similar interhemispheric disparity in the amount of activated chlorine has been seen in OClO slant column abundances [*Miller et al.*, 1999; *Wagner et al.*, 2001]. We will return to this point below.

[13] Figure 1 also shows that, in keeping with the greater degree of interannual variability in the meteorological conditions that govern PSC formation and hence chlorine activation, the Arctic exhibits much more variation in the magnitude and distribution of ClO enhancement than does the Antarctic. A larger degree of variability in the magnitude and timing of chlorine activation in the Arctic than in the Antarctic has also been seen in the multi-year OClO data set from the Global Ozone Monitoring Experiment (GOME) satellite instrument [*Wagner et al.*, 2001]. Nevertheless, with the exception of the comparatively mild winter of 1997/1998 (not shown), in all years in which MLS had adequate data coverage, the Arctic vortex was observed to be almost completely filled with enhanced ClO in midwinter to late winter.



0.15 0.45 0.75 1.05 1.35 1.65 1.95
CLO / ppbv

[14] It should be emphasized that the minimum temperature attained in any given winter is not the sole factor controlling CIO abundances: The position of the low-temperature area with respect to the region of strongest winds and the general placement of the vortex also significantly affect the amount of air that can undergo chemical processing. For instance, as discussed by *Waters et al.* [1995], temperatures below PSC existence thresholds were present in the Arctic in late December 1992, but they were located near the vortex center where both winds and insolation were relatively weak; as a result, CIO enhancement in early January 1993 (not shown) was smaller than during the same period in 1992 (Figure 1), when minimum temperatures occurred in a region that experienced both sunlight and strong winds [*Waters et al.*, 1993b]. In February 1993, however, the low-temperature region was situated near the vortex edge where winds and sunlight were stronger, and the vortex was filled with enhanced CIO (Figure 1). The coldest period of the 1993/1994 Arctic winter occurred in late February/early March; although mostly sunlit, the vortex at this time (Figure 1) was not so completely filled with high CIO as it had been in January 1992 or February 1993 because the low temperatures were confined to the vortex interior where winds were weaker. In February 1995, the vortex and the low-temperature region were substantially shifted off the pole, increasing the fraction of the vortex illuminated by sunlight and enhancing CIO production (note that minimum temperatures had just risen above 194 K at 520 K on 8 February [*Manney et al.*, 1996a], the day depicted in Figure 1). An extensive region of low temperatures along the vortex edge in January 1996 led to very high CIO values, particularly at 520 K. Later that winter, in mid-February and again in early March (not shown), strong tropospheric ridging events also created situations in which regions of very low temperatures straddled the vortex edge and CIO values were high throughout most of the vortex [*Santee et al.*, 1996a]. Although temperatures were also low in February 1997, the location of the cold region further away from the jet core enabled less processing of air than in 1996 [*Santee et al.*, 1997], especially at 520 K.

[15] Not only were the cold regions situated near the vortex edge in the Arctic late winters of 1992, 1993, and 1996, but also the variations in the vortex shape and location and in the relative positions of the vortex and cold pool were larger and more rapid than in, for example, 1994

or 1997. These conditions all contribute to the vortex being more completely filled with enhanced CIO. That the vortex core becomes filled with high CIO during active conditions, even when the cold region is near the vortex edge and does not extend to its center, suggests that mixing within the vortex is also enhanced at these times.

[16] The behavior in the north is in strong contrast with that in the south, where at 465 K the region of low temperatures extends nearly out to the vortex edge and the CIO is more uniformly enhanced in every year. At 520 K, however, although the cold region encompasses a large area (much larger than in the Arctic), it is typically smaller than and nearly concentric with the area of the vortex itself, and thus the low temperatures are often situated well back from the vortex edge. In addition, the vortex tends to be less variable (i.e., more constant in shape and position) in the south [e.g., *Andrews*, 1989; *Waugh and Randel*, 1999; *Waugh et al.*, 1999], with little large-scale mixing between the core and edge regions [e.g., *Schoeberl et al.*, 1992; *Bowman*, 1993; *Lee et al.*, 2001]. As a consequence, during comparable periods the vortex can be less completely filled with enhanced CIO at this level in the Antarctic than in the Arctic. We will explore this point further in connection with Figure 2.

[17] Finally, Figure 1 also shows that, for the most part, enhanced CIO is confined within the winter polar vortex. A steep gradient in CIO and OCIO abundances has been observed in the vicinity of the vortex boundary in aircraft data [e.g., *Brune et al.*, 1989, 1990; *Schiller et al.*, 1990], and ground-based measurements have also indicated sharp changes in CIO and OCIO at both polar [e.g., *de Zafra et al.*, 1995; *Kreher et al.*, 1996] and midlatitude [*Gerber and Kämpfer*, 1994] stations as the vortex wobbled about overhead. The importance of atmospheric motions in controlling the distribution of enhanced CIO is most easily illustrated, however, in the hemispheric maps obtained by a satellite instrument. As noted initially by *Waters et al.* [1993b], the high CIO region observed by MLS is generally bounded on the poleward side by the edge of daylight and on the equatorward side roughly by the edge of the vortex (taken here to be the $0.25 \times 10^{-4} \text{ K m}^2 \text{ kg}^{-1} \text{ s}^{-1}$ contour of potential vorticity (PV) at 465 K and $0.40 \times 10^{-4} \text{ K m}^2 \text{ kg}^{-1} \text{ s}^{-1}$ at 520 K). The occasional slightly elevated values of CIO measured by MLS at low latitudes and midlatitudes (outside of the polar vortex) have been shown in large part to be statistically consistent with measurement noise

Figure 1. (opposite) Maps of MLS CIO at 465 K (left) and 520 K (right) for one day during each of six winters in both the Southern (left column) and Northern (right column) Hemispheres. MLS data from both ascending and descending sides of the orbit were gridded and vertically interpolated to potential temperature surfaces using analyzed temperatures from the U.K. Met Office [*Swinbank and O'Neill*, 1994]. Only data taken at local solar zenith angle (SZA) $< 88^\circ$ (daylight) are shown; blank spaces represent areas where data are missing or have been screened out with the SZA criterion. Two contours of Met Office potential vorticity (PV) are shown in white on each map to indicate the approximate size and strength of the polar vortex (see text). Different contours of Met Office temperature are shown in black to indicate the approximate existence thresholds for nitric acid trihydrate (NAT) polar stratospheric clouds under various conditions. In the Northern Hemisphere, the contours represent 196 K and 194 K at 465 K and 520 K, respectively; these values were calculated by using the formula of *Hanson and Mauersberger* [1988] and assuming a HNO_3 mixing ratio of 12 ppbv, a H_2O mixing ratio of 5 ppmv, and a pressure of 50 hPa (35 hPa) at 465 K (520 K). In the Southern Hemisphere, where lower temperatures mean that the pressures corresponding to the potential temperature surfaces are lower and the stratosphere is severely denitrified ($\text{HNO}_3 = 1$ ppbv) and dehydrated ($\text{H}_2\text{O} = 2.5$ ppmv) in mid-to-late August, the values are 189 K and 187 K at 465 K and 520 K, respectively.

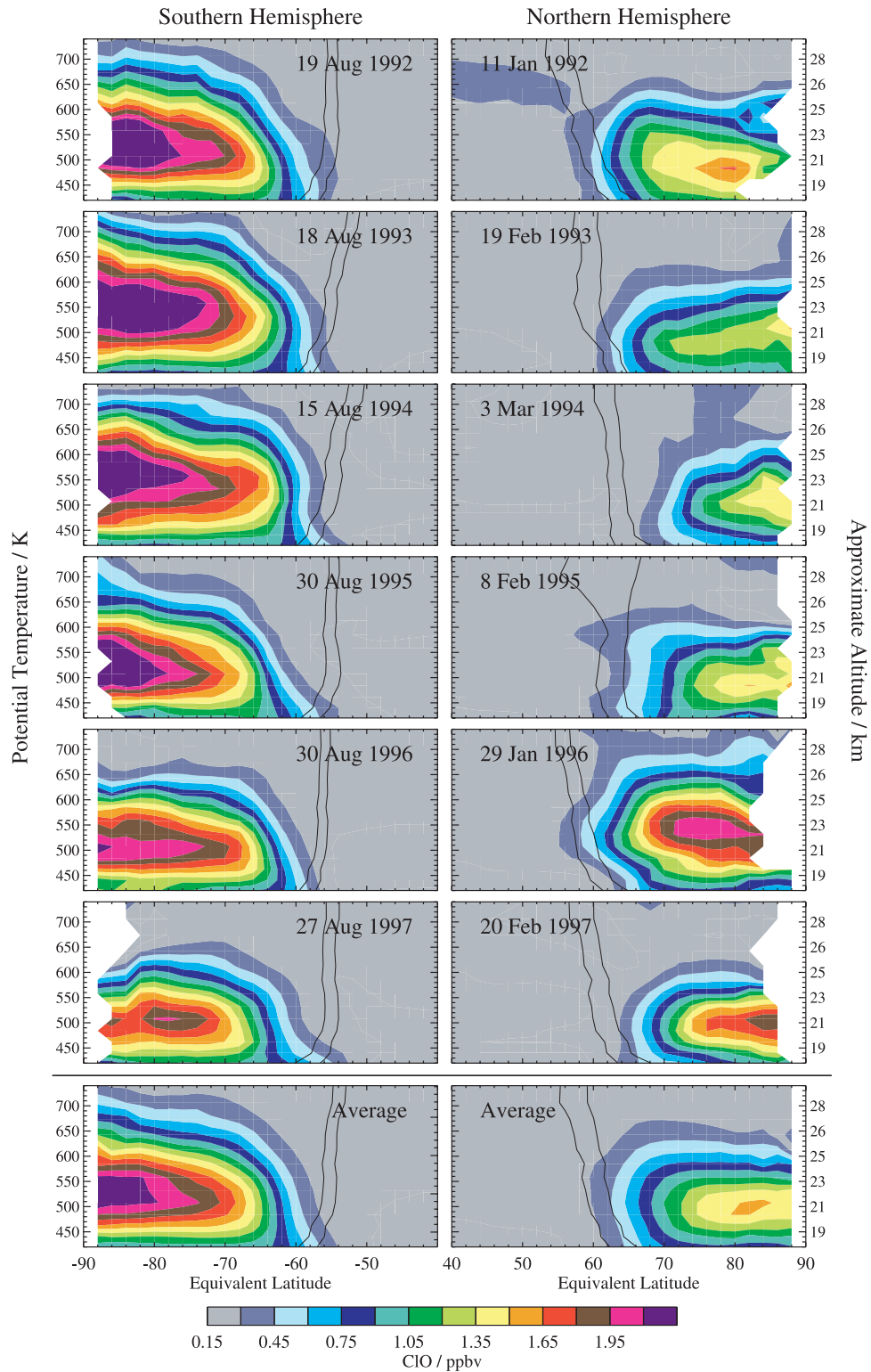


Figure 2. Equivalent latitude/potential temperature (EqL/ θ) cross sections of MLS CIO for the same days as shown in Figure 1. Only data taken at SZA $< 88^\circ$ (daylight) are included in the averages. The black lines represent approximately the same two PV contours as on the maps in Figure 1, but scaled to give similar values throughout the θ domain. The approximate altitude scale is calculated using the nonlinear formula of *Knox* [1998]. The bottom panels show distributions obtained by averaging together the data from the individual days plotted above.

[Schoeberl *et al.*, 1993]. Although some of these patches may represent the remnants of small blobs of air that have been spun off of the vortex, in general there appears to be little leakage of processed air during the midwinter to late winter periods represented here (at least at the spatial scales discernable in the MLS data). This finding is consistent with the results of recent modeling studies [e.g., Li *et al.*, 2002; Öllers *et al.*, 2002, and references therein] showing that the Antarctic vortex is highly isolated in August and September. Similarly, Norton and Chipperfield [1995] have shown that, although exchange between the vortex and midlatitudes is greater in the Arctic, and there is a large degree of interannual variation in the permeability of the vortex, in general large amounts of PSC-activated air are not exported to lower latitudes.

[18] We next investigate the vertical distribution of enhanced CIO by examining equivalent latitude/potential temperature (EqL/ θ) representations. (EqL is the latitude that would enclose the same area between it and the pole as a given PV contour [e.g., Butchart and Remsberg, 1986].) Figure 2 shows that, typically, the magnitude of the maximum CIO abundances and their horizontal and vertical extent are considerably larger in the Antarctic than in the Arctic. Figure 2 also shows that the peak in the CIO profile typically falls in the range 500–550 K (~ 21 – 23 km) in the Antarctic but 480–500 K (~ 20 – 21 km) in the Arctic. The exception to this general rule occurred in the Arctic winter of 1995/1996, when the altitude of the maximum CIO mixing ratio was about 550 K, higher than during the Southern Hemisphere winter that year. The interhemispheric difference in the CIO profile peak altitudes observed by MLS is contrary to what has been reported from other data sets. For example, on the basis of the fact that the relative increase in OCIO slant column amounts with SZA is nearly identical in the Arctic and the Antarctic, Wagner *et al.* [2001] concluded that the height of the maximum OCIO concentration is similar in both hemispheres. This approach yields fairly poor height discrimination, however, and a difference of only a few kilometers in the altitude of the profile peak may not be discernible in the column abundances. In reporting ground-based millimeter-wave CIO observations from Ny Ålesund, Raffalski *et al.* [1998] asserted that the lower stratospheric Antarctic CIO maximum is usually found at lower altitudes than that in the Arctic. Shindell *et al.* [1994], Emmons *et al.* [1995], de Zafra *et al.* [1995], Klein *et al.* [1996], Nagar *et al.* [1999] and Solomon *et al.* [2000, 2002] have all reported, for various years, peak altitudes of ~ 19 – 20 km for Antarctic profiles during September, while Shindell *et al.* [1994] and Nagar *et al.* [1999] have reported similar altitudes for the profile peak in the Arctic. The apparent discrepancy with MLS in the height of the CIO peak may arise simply from the timing of the ground-based measurements: Both de Zafra *et al.* [1995] and Solomon *et al.* [2000, 2002] show Antarctic peak altitudes that are slightly higher (21–22 km) in late August/early September and decline steadily thereafter. The decrease in the height of the maximum mixing ratio during the winter will be discussed further in the next section.

[19] Not only is the MLS CIO profile peak usually slightly higher in the Antarctic, but the vertical extent of chlorine activation is also larger (up to 700 K or above in

some years) than in the Arctic (typically not much above 600 K). Enhanced CIO abundances often reach to lower altitudes in the Antarctic as well. Wagner *et al.* [2001, 2002] proposed two different explanations for the substantial ($\sim 40\%$) interhemispheric differences in OCIO slant column densities observed by GOME: smaller maximum CIO abundances in the Arctic, or, assuming that CIO peak values are similar in both hemispheres, a smaller altitude range over which chlorine is activated in the Arctic. On the basis of MLS observations [e.g., Waters *et al.*, 1993b; Santée *et al.*, 1995] showing comparable maximum CIO abundances in both polar vortices, Wagner *et al.* [2001, 2002] concluded that the vertical extent of chlorine activation must be smaller in the Arctic. The papers reporting the MLS observations, however, focused on the 465 K level in the stratosphere, where the disparity between maximum CIO mixing ratios in the Arctic and Antarctic is relatively small. Therefore it is likely that both of the proposed explanations contribute to the differences seen in the OCIO column amounts. By examining variations in the correlation between OCIO slant columns and minimum temperatures at various levels in the lower stratosphere, Wagner *et al.* [2001] further concluded that chlorine activation is limited primarily to the layer between 400 and 475 K in the Arctic. The MLS data in Figure 2 indicate a much broader extent for CIO enhancement in the Arctic.

[20] In keeping with the greater size of the Antarctic vortex [Waugh and Randel, 1999], CIO enhancement typically extends 5– 10° in EqL further equatorward in the Antarctic than in the Arctic. At the lowest levels, enhanced CIO fills the vortex to a similar extent in both hemispheres. From ~ 470 – 600 K, however, the vortex is usually more completely filled with high CIO in the Arctic. As discussed in detail in connection with Figure 1, differences in the altitude structure of enhanced CIO in the two hemispheres, as well as the large degree of interannual variability in the Arctic, reflect variations in the shape and location of the vortex, the relative positions of the vortex and cold regions, and the strength of the mixing within the vortex. In general, CIO enhancement extends farther out when the cold region is situated along the vortex edge, although the largest CIO abundances are still typically located deep in the vortex interior.

[21] In both Figures 1 and 2, the Arctic winter of 1995/1996 stands out as producing a much more Antarctic-like CIO distribution than usual, with larger maximum CIO abundances (almost 2 ppbv), a higher altitude for the profile peak (~ 550 K), and greater horizontal and vertical (up to 650 K) extent of activation. This pattern is consistent with the greater extent and duration of temperatures below PSC existence thresholds [e.g., Pawson and Naujokat, 1999] and larger decrease in lower stratospheric ozone [e.g., Manney *et al.*, 2003] in this year.

4. Overview of CIO Mean Evolution

[22] In this section we examine different sets of time series to track the mean evolution of CIO over complete annual cycles in both hemispheres. As mentioned in section 2.1, during a short interval in the middle of every UARS month MLS makes measurements only in darkness; as a consequence, MLS observes CIO abundances to briefly dip and

then increase again as orbit precession brings measurements into stronger sunlight. Thus the particulars of the measurement geometry can cause an artificial minimum in measured CIO values. In order to mitigate this effect in the time series plots presented in this section, we have imposed a fairly strict constraint on the local solar time (LST) of the measurements, in addition to the SZA screening used in the previous plots. Modeling results, for example those of *Shindell and de Zafra* [1996] for the 20-km level over McMurdo Station in early and mid-September, indicate that CIO abundances are at their peak values between the hours of about 12:00 and 13:00. By restricting the LST of the MLS measurements to within an hour on either side of this interval, we obtain midday averaged CIO values that are representative of the actual levels of active chlorine. Therefore, for the time series plots shown here, only measurements satisfying both solar zenith angle ($SZA < 88^\circ$) and local solar time ($11:00 < LST < 14:00$) criteria are included in the averages.

[23] We begin by binning the data into 5° EqL bands and averaging; results are shown in Figure 3 for seven years in both the Arctic and the Antarctic at 520 and 465 K. Again, as seen in the previous section, CIO enhancement exhibits much greater interannual variability in the Arctic than in the Antarctic. Note that variations in the geographical sampling of an inherently inhomogeneous field can give rise to significant day-to-day scatter in these plots. In addition, the more frequent distortions and elongations of the vortex in the Arctic lead to greater data coverage in sunlit conditions at high equivalent latitudes in early winter than in the Antarctic, where, for example, in June very few points appear on the plots for the highest EqL bands. It is still clear, however, that CIO in the sunlit portions of the southern hemispheric vortex becomes enhanced (>0.5 ppbv) by at least late May/early June every year at these levels, with the earliest detection constrained by the UARS yaw cycle and other operational considerations. (Figure 7 of *Waters et al.* [1999] shows maps of the earliest MLS measurements of enhanced Antarctic CIO for 1992–1997.) Consistent with the first appearance of large abundances of active chlorine, Antarctic ozone depletion has been shown to start in June at the sunlit vortex edge and then follow the terminator as it sweeps poleward over the course of the winter [*Manney et al.*, 1995; *Roscoe et al.*, 1997; *Lee et al.*, 2000]. In the north, CIO becomes enhanced in mid to late December in some years but not until January in others, following the onset of temperatures low enough for PSC formation. The MLS data are in accord with aircraft measurements showing that the air inside the Arctic vortex was already highly activated by early January in 1989 [*Brune et al.*, 1990] and by mid-December in 1991 [*Toohey et al.*, 1993]. Similar timing is also seen for the onset of enhanced OCIO in both hemispheres [*Miller et al.*, 1999; *Wagner et al.*, 2001]. MLS observations of enhanced Arctic CIO are also consistent with recent findings based on several independent data sets indicating the occurrence of significant early winter and midwinter ozone loss [e.g., *Deniel et al.*, 1998; *Becker et al.*, 2000; *Manney et al.*, 2003; *Rex et al.*, 2003].

[24] In general the highest CIO abundances occur near the highest equivalent latitudes in the vortex core. MLS registered the largest Arctic CIO abundances in late January/

February 1993, 1996, and 1997, cold years with temperatures continuously below PSC thresholds for long periods, and the smallest in 1998, when the vortex was relatively warm; these results are qualitatively consistent with the amount of chemical ozone depletion estimated from the MLS ozone data in these years [*Manney et al.*, 2003]. Maximum CIO values are up to ~ 0.5 ppbv ($\sim 25\%$) larger in the Antarctic than in the Arctic at 520 K (~ 1.0 ppbv, or ~ 60 – 70% , larger at 585 K, not shown), but not at 465 K, where peak abundances are roughly comparable in the two hemispheres. OCIO slant column densities from GOME indicate differences as large as 40% in the peak values in the two hemispheres [*Wagner et al.*, 2001]; as discussed in the previous section, at least part of this interhemispheric disparity is attributable to differences in active chlorine concentrations. *Miller et al.* [1999] also report ground-based OCIO slant columns that are 30–50% larger in the Antarctic than in the Arctic.

[25] Figure 3 shows that in the north, the largest CIO values are observed in January or February, depending on the year. In the south, observed mixing ratios typically reach peak values in August and then decrease slightly or remain relatively constant into early to mid-September. It should be noted, however, that CIO abundances may have been still increasing when the midyaw period interval of nighttime-only measurements (which occurred ~ 5 days earlier in each successive year) began; thus it is possible that MLS failed to observe the actual peak values in some or all of the years. Ground-based measurements from McMurdo Station show CIO abundances decreasing at these levels from the start of the observing periods in early September 1993 [*de Zafra et al.*, 1995] and 1994 [*Klein et al.*, 1996], and measurements from Arrival Heights show stratospheric OCIO columns remaining fairly constant from the beginning of the observing period in late August until mid-September 1993 [*Kreher et al.*, 1996]. However, other ground-based measurements of CIO from Scott Base over 1996–2000 [*Solomon et al.*, 2002] and OCIO from McMurdo in 1991, 1993, and 1996 [*Miller et al.*, 1999] indicate that maximum chlorine activation occurred in early September rather than in August. On the basis of satellite measurements, *Wagner et al.* [2001] also report that chlorine activation reaches its maximum by mid-September, but inspection of their Plate 5 reveals that only in 1995 and 1999 did peak OCIO slant columns occur in mid-September; in 1996, 1997, and 1998, maximum OCIO amounts were recorded in mid-August. Thus the observational records from different instruments/locations do not provide a consistent picture on this issue, although some of the apparent inconsistencies may arise from interannual or spatial variability. In any case, operational constraints prevented MLS from precisely identifying the time of greatest chlorine activation in any given year.

[26] In the Arctic, the timing of the start of chlorine deactivation varies widely, but it is typically completed by mid-March. An exception to this general rule occurred in the spring of 1997, when the lower stratospheric vortex was unusually cold and long-lived. Unfortunately, a UARS yaw maneuver prevented MLS from viewing northern high latitudes past the end of February in this winter; when MLS turned back north on 10 April, chlorine had been deactivated [*Santee et al.*, 1997]. Observations from GOME [*Wagner et al.*, 2001] and a ground-based instrument at Ny

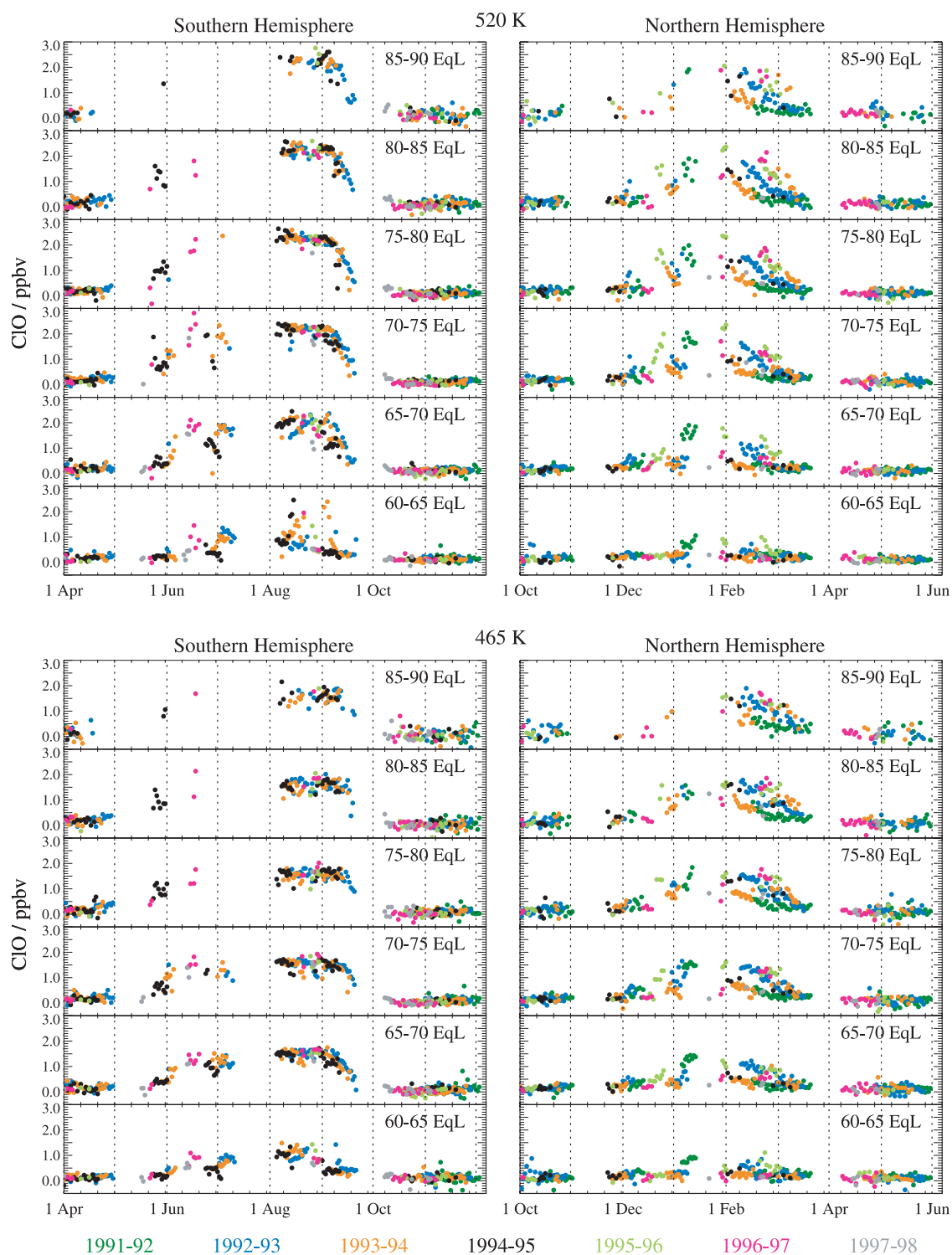


Figure 3. Time series of MLS CIO at 520 K (top) and 465 K (bottom) for both the Southern (left) and Northern (right) Hemispheres. Measurements were binned into 5° EqL bands and averaged; only data taken near midday (i.e., having local SZA $< 88^\circ$ and local solar time (LST) between 11:00 and 14:00) were included in the averages. Different years are represented by different colors as indicated in the legend. The x-axis tick mark increment is 10 days; dotted vertical lines demark calendar months. For the averages shown here, the precision is ~ 0.2 ppbv for the 85–90 EqL bin (where 2–3 data points typically contribute to each daily average) and ~ 0.1 ppbv for the 65–70 EqL bin (where about 10 data points typically contribute to each daily average).

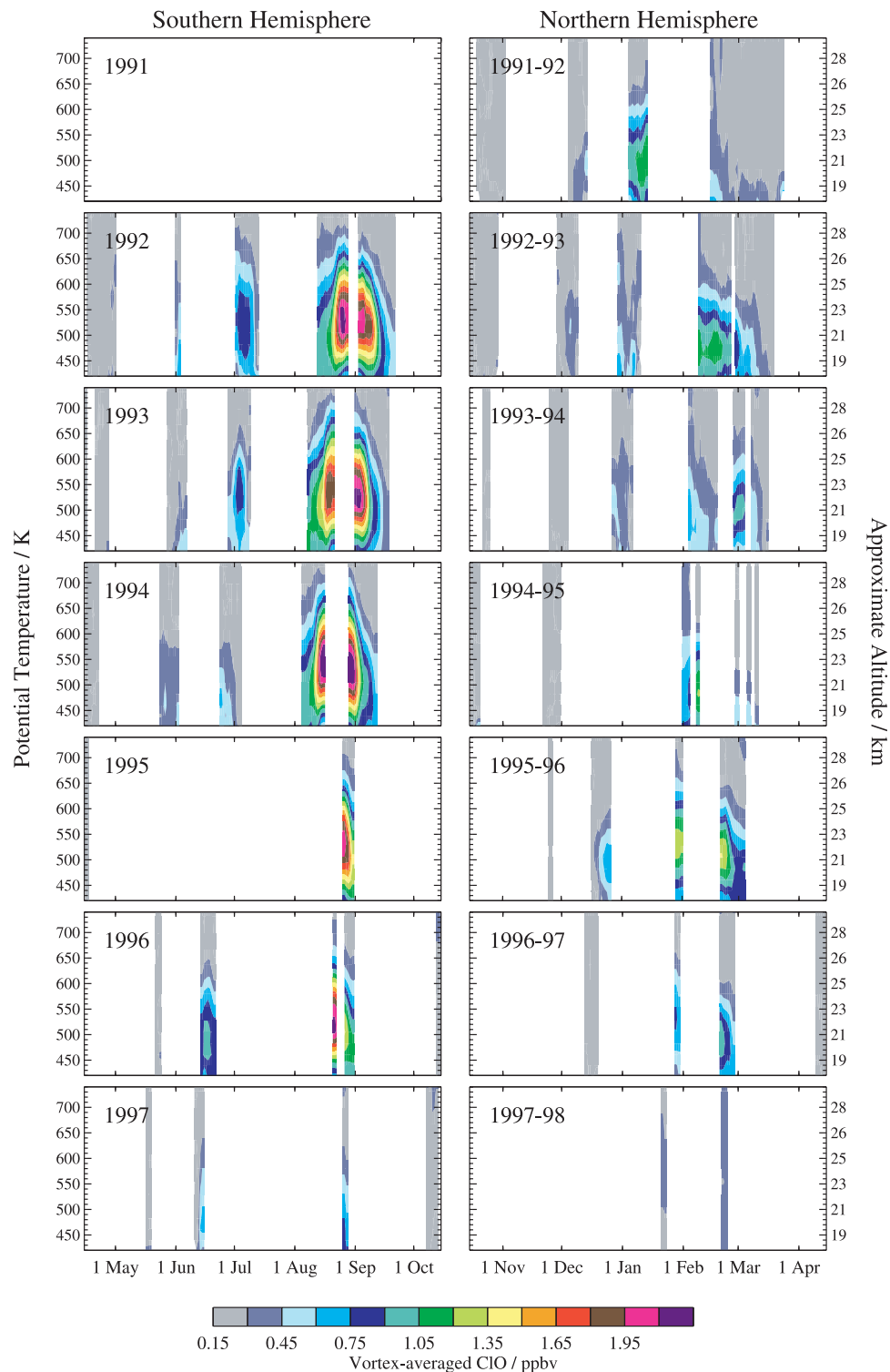


Figure 4. Vortex-averaged MLS CIO, calculated within the $1.2 \times 10^{-4} \text{ s}^{-1}$ contour of “scaled” PV (where scaled PV, which has roughly the same values on isentropic surfaces throughout the stratosphere, was calculated using the method of *Manney et al.* [1994a]), as a function of potential temperature and time for the Southern (left) and Northern (right) Hemispheres. Only data taken at $\text{SZA} < 88^\circ$ and $11:00 < \text{LST} < 14:00$ (midday) are included in the averages.

Ålesund [*Raffalski et al.*, 1998], however, indicate that chlorine was still activated in late March 1997, in keeping with the persistence of temperatures below PSC existence thresholds [e.g., *Coy et al.*, 1997]. In contrast, in the

Antarctic CIO consistently remains enhanced in mid-September, especially at 465 K (the rate of decline in CIO appears steeper at 520 K). The interruption in high-latitude coverage, together with the decreasing measurement

frequency toward the end of the mission, precluded observation of the complete recovery period in the south in any year. By the time MLS measurements at high southern latitudes resume in mid-October, chlorine has been deactivated. Other measurements of CIO [e.g., *Shindell et al.*, 1994; *de Zafra et al.*, 1995; *Wehr et al.*, 1995; *Solomon et al.*, 2000, 2002] and OCIO [e.g., *Kreher et al.*, 1996; *Miller et al.*, 1999; *Wagner et al.*, 2001] indicate times for chlorine deactivation in both hemispheres that are similar to those from MLS. Thus elevated levels of reactive chlorine persist for 4–5 months in the south but only 2–3 months in the north.

[27] Figure 4 shows time series of vortex-averaged CIO as a function of potential temperature for seven years. Small data gaps in these plots have been filled by running the daily vortex averages through a Kalman smoother. Blank spaces appear where the error in the interpolated values exceeds a certain threshold, indicating that the interval is too far from existing measurements. Such blank spaces arise not only during the times when MLS has yawed away to observe the opposite hemisphere, but also in the middle of observation periods when MLS makes measurements only in darkness. As discussed earlier, CIO enhancement extends over a larger vertical range and persists for a longer period of time in the Southern Hemisphere than in the Northern Hemisphere. Interestingly, after peak CIO mixing ratios are attained in August in the Antarctic and January/February in the Arctic, the altitude of the peak is observed to move downward as the winter progresses. This is consistent with the pattern of stratospheric temperatures [e.g., *Manney et al.* 1996b] and the overall downward trend in PSC altitude observed over the course of the winter in both hemispheres [e.g., *Poole and Pitts*, 1994; *Fromm et al.*, 1999]. Continued downward transport through September may also contribute to the drop in peak altitude, as noted by *de Zafra et al.* [1995], who observed a similar monotonic drift downward in the altitude of the peak in ground-based CIO measurements taken during September, as did *Solomon et al.* [2000, 2002]. Since the region of high CIO decays from the top down, chlorine remains activated for a much longer duration at the lower levels.

[28] Finally, we present in Figure 5 climatologies of MLS CIO as a function of EqL and time at five θ levels ranging between 655 and 420 K. These climatologies have been derived by averaging together the results for seven individual years at each level. Because a given UARS month starts about 5 days earlier in each succeeding year, many of the data gaps visible in the previous time series plots are shortened when several years of measurements are averaged together; this is particularly true in the Arctic, where a larger degree of variability in the shape and location of the vortex leads to greater data sampling in sunlit conditions at high equivalent latitudes. Averaging does not remove the data gaps entirely, however, so to eliminate breaks in the climatological fields, Kalman smoothing has been applied to the averaged CIO values at each level. In order to ensure that one anomalous day/year does not dominate the climatological fields, a greater degree of smoothing has been applied to these averages than was used in Figure 4. Unlike in Figure 4, where intervals far from actual midday measurements were blanked out, in the climatologies shown in Figure 5, the regions in which the estimated precision of the interpolated values is poor are denoted by paler colors. These climatol-

ogies encapsulate many of the general patterns in enhanced CIO noted earlier: e.g., the much greater horizontal and vertical extent, duration, and magnitude of chlorine activation in the Antarctic than in the Arctic.

5. Summary and Conclusions

[29] UARS MLS measurements of stratospheric CIO over seven annual cycles in both hemispheres were presented to provide an overview of the interhemispheric and interannual variations in the distribution of active chlorine, in particular the evolution of enhanced CIO in the lower stratospheric winter polar vortices. Daily maps and equivalent latitude/potential temperature cross sections were used to show interhemispheric and interannual differences in wintertime CIO abundances, and time series of different slices through the data were examined to develop a comprehensive picture of the mean evolution of enhanced vortex CIO. In some cases climatological fields were derived by averaging together the results for individual years. The main conclusions of this work are as follows:

[30] 1. At 465 K, which is the level that most previous studies reporting MLS CIO data focused on, CIO enhancement within the Arctic vortex is fairly comparable in both magnitude and spatial extent to that in the Antarctic. At 520 K (585 K), however, maximum CIO abundances are as much as ~ 0.5 ppbv (~ 1.0 ppbv) larger in the Antarctic than in the Arctic, and the spatial extent of activated chlorine is significantly greater.

[31] 2. The Arctic exhibits much more interannual variability in the magnitude, timing, and horizontal and vertical extent of CIO enhancement than does the Antarctic. Nevertheless, MLS observed the Arctic vortex to be almost completely filled with enhanced CIO during the cold winters of the mid-1990s.

[32] 3. The peak in the CIO profile typically falls in the range 500–550 K (~ 21 – 23 km) in the Antarctic but 480–500 K (~ 20 – 21 km) in the Arctic, and the vertical extent of chlorine activation is also larger in the Antarctic (up to 700 K or above in some years) than in the Arctic (typically not much above 600 K). Enhanced CIO abundances often reach to lower altitudes in the Antarctic as well.

[33] 4. The Arctic winter of 1995/1996 stands out as having a much more Antarctic-like CIO distribution, with larger maximum CIO abundances (almost 2 ppbv), a higher altitude for the profile peak (~ 550 K), and greater horizontal and vertical (up to 650 K) extent of activation than the other winters observed by MLS.

[34] 5. In the Southern Hemisphere, CIO becomes enhanced in the sunlit portions of the vortex by at least late May/early June every year, whereas in the Northern Hemisphere CIO becomes enhanced in mid to late December in some years but not until January in others. In the Arctic, chlorine deactivation is typically completed by mid-March. In contrast, in the Antarctic CIO consistently remains enhanced in mid-September, especially at 465 K. Thus elevated levels of reactive chlorine persist for 4–5 months in the south but only 2–3 months in the north.

[35] Current and planned future measurements should continue to improve our understanding of stratospheric chlorine. The Submillimetre Radiometer (SMR) and Optical Spectrograph and InfraRed Imaging System (OSIRIS)

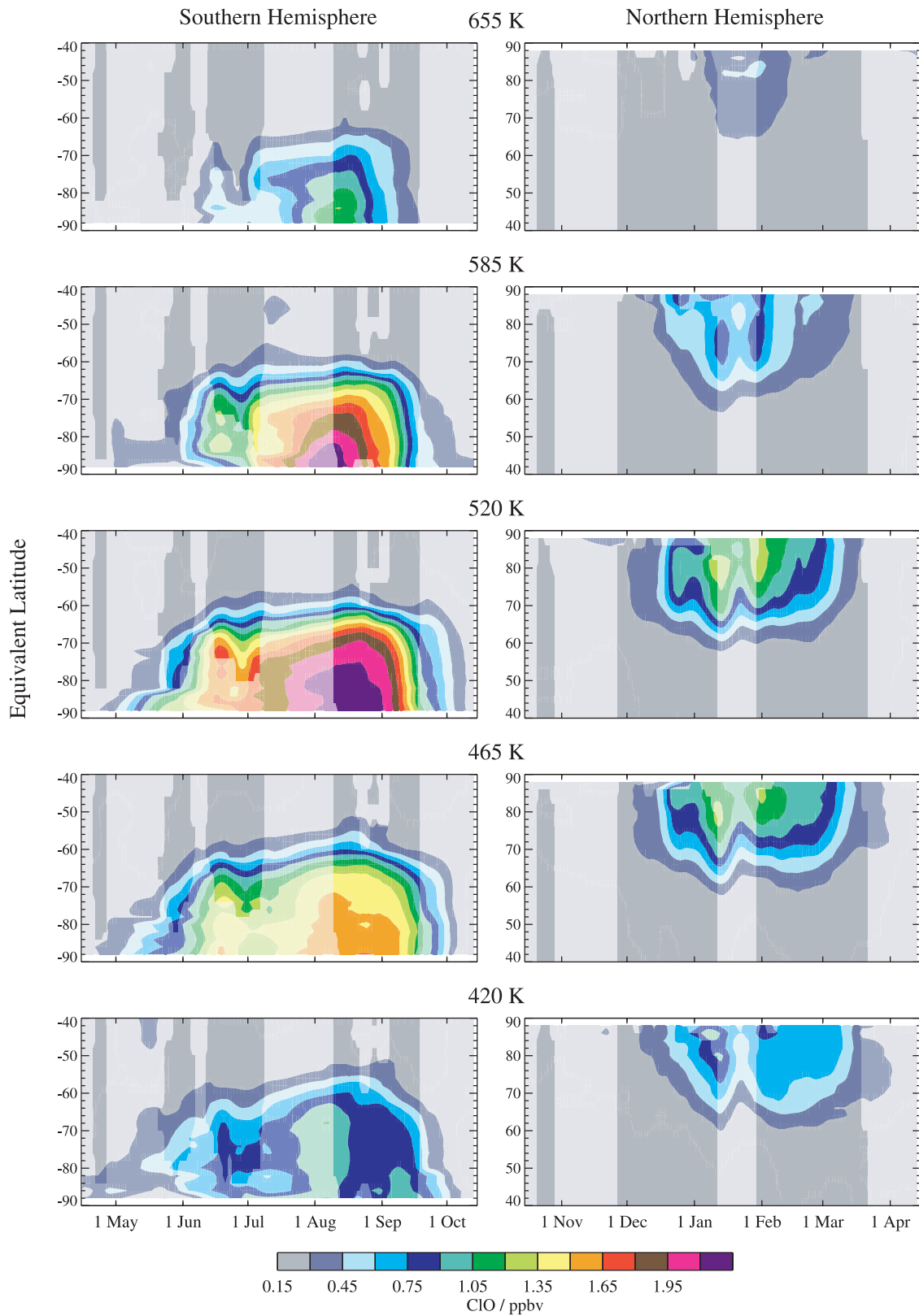


Figure 5. Climatologies of midday ($SZA < 88^\circ$, $11:00 < LST < 14:00$) MLS CIO as a function of EqL and time at five potential temperature levels between 655 K (top panel) and 420 K (bottom panel), derived by averaging together the results for seven individual years at each level. To fill in breaks in the climatological fields arising from data gaps, Kalman smoothing has been applied to the averaged CIO values at each level; paler colors denote regions where the estimated precision of the interpolated values is poor.

instruments on board the Odin satellite, launched in February 2001, make global measurements of ClO and OClO profiles, respectively. The Scanning Imaging Absorption Spectrometer for Atmospheric Cartography (SCIAMACHY), with heritage from GOME, was launched in early 2002 and obtains stratospheric column and some profile information for both ClO and OClO under enhanced polar conditions. The Ozone Monitoring Instrument (OMI), to be launched in early 2004 as part of NASA's Earth Observing System (EOS) Aura mission, will provide OClO column measurements. The Aura payload will also include an enhanced version of the MLS instrument [Waters *et al.*, 1999]. Many of the measurement shortcomings that hampered this study will be ameliorated with the new instrument. For example, EOS MLS will perform measurements with the instrument fields of view scanning the limb in the orbit plane to provide latitudinal coverage that will extend from 82°N to 82°S on every orbit, affording continuous monitoring of the polar regions (no monthly gaps arising from yaw maneuvers as on UARS). In addition, EOS MLS ClO measurements will have improved vertical and horizontal resolution and significantly (by about a factor of two) better precision. Finally, because the Aura orbit will be sun-synchronous, MLS observations at a given latitude on either the ascending or descending sides of orbit will have the same local solar time throughout the mission, eliminating the intervals of nighttime-only measurements that arose in the middle of each UARS yaw cycle.

[36] **Acknowledgments.** We thank L. Froidevaux for very helpful comments and the U.K. Met Office (especially R. Swinbank) for meteorological analyses. We also thank the two anonymous reviewers for their suggestions. Work at the Jet Propulsion Laboratory, California Institute of Technology, was done under contract with the National Aeronautics and Space Administration.

References

- Andrews, D. G., Some comparisons between the middle atmosphere dynamics for the Southern and Northern Hemispheres, *Pure Appl. Geophys.*, **130**, 213–232, 1989.
- Avallone, L. M., D. W. Toohey, W. H. Brune, R. J. Salawitch, A. E. Dessler, and J. G. Anderson, Balloon-borne in situ measurements of ClO and ozone: Implications for heterogeneous chemistry and mid-latitude ozone loss, *Geophys. Res. Lett.*, **20**, 1795–1798, 1993.
- Barath, F. T., et al., The Upper Atmosphere Research Satellite Microwave Limb Sounder Instrument, *J. Geophys. Res.*, **98**, 10,751–10,762, 1993.
- Becker, G., R. Müller, D. S. McKenna, M. Rex, K. S. Carslaw, and H. Oelhaf, Ozone loss rates in the Arctic stratosphere in the winter 1994/1995: Model simulations underestimate results of the Match analysis, *J. Geophys. Res.*, **105**, 15,175–15,184, 2000.
- Bormann, S., S. Solomon, J. E. Dye, and B. P. Luo, The potential of cirrus clouds for heterogeneous chlorine activation, *Geophys. Res. Lett.*, **23**, 2133–2136, 1996.
- Bormann, S., S. Solomon, J. E. Dye, D. Baumgardner, K. K. Kelly, and K. R. Chan, Heterogeneous reactions on stratospheric background aerosols, volcanic sulfuric acid droplets, and type I polar stratospheric clouds: Effects of temperature fluctuations and differences in particle phase, *J. Geophys. Res.*, **102**, 3639–3648, 1997.
- Bowman, K. P., Large-scale isentropic mixing properties of the Antarctic polar vortex from analyzed winds, *J. Geophys. Res.*, **98**, 23,013–23,027, 1993.
- Brune, W. H., J. G. Anderson, and K. R. Chan, In situ observations of ClO in the Antarctic: ER-2 aircraft results from 54°S to 72°S latitude, *J. Geophys. Res.*, **94**, 16,649–16,663, 1989.
- Brune, W. H., D. W. Toohey, J. G. Anderson, and K. R. Chan, In situ observations of ClO in the Arctic stratosphere: ER-2 aircraft results from 59°N to 80°N latitude, *Geophys. Res. Lett.*, **17**, 505–508, 1990.
- Butchart, N., and E. E. Remsberg, The area of the stratospheric polar vortex as a diagnostic for tracer transport on an isentropic surface, *J. Atmos. Sci.*, **43**, 1319–1339, 1986.
- Coy, L., E. R. Nash, and P. A. Newman, Meteorology of the polar vortex: Spring 1997, *Geophys. Res. Lett.*, **24**, 2693–2696, 1997.
- Deniel, C., R. M. Bevilacqua, J. P. Pommereau, and F. Lefèvre, Arctic chemical ozone depletion during the 1994–1995 winter deduced from POAM II satellite observations and the REPROBUS three-dimensional model, *J. Geophys. Res.*, **103**, 19,231–19,244, 1998.
- Dessler, A. E., et al., Balloon-borne measurements of ClO, NO, and O₃ in a volcanic cloud: An analysis of heterogeneous chemistry between 20 and 30 km, *Geophys. Res. Lett.*, **20**, 2527–2530, 1993.
- de Zafra, R. L., J. M. Reeves, and D. T. Shindell, Chlorine monoxide in the Antarctic spring vortex. 1. Evolution of midday vertical profiles over McMurdo Station, 1993, *J. Geophys. Res.*, **100**, 13,999–14,007, 1995.
- Douglass, A. R., M. R. Schoeberl, R. S. Stolarski, J. W. Waters, J. M. Russell III, A. E. Roche, and S. T. Massie, Interhemispheric differences in springtime production of HCl and ClONO₂ in the polar vortices, *J. Geophys. Res.*, **100**, 13,967–13,978, 1995.
- Emmons, L. K., D. T. Shindell, J. M. Reeves, and R. L. de Zafra, Stratospheric ClO profiles from McMurdo Station, Antarctica, spring 1992, *J. Geophys. Res.*, **100**, 3049–3055, 1995.
- Froidevaux, L., J. W. Waters, W. G. Read, P. S. Connell, D. E. Kinnison, and J. M. Russell III, Variations in the free chlorine content of the stratosphere (1991–1997): Anthropogenic, volcanic, and methane influences, *J. Geophys. Res.*, **105**, 4471–4481, 2000.
- Fromm, M. D., R. M. Bevilacqua, J. Hornstein, E. P. Shettle, K. Hoppel, and J. D. Lumpe, An analysis of Polar Ozone and Aerosol Measurement (POAM) II Arctic stratospheric cloud observations, 1993–1996, *J. Geophys. Res.*, **104**, 24,341–24,357, 1999.
- Gerber, L., and N. Kämpfer, Millimeter-wave measurements of chlorine monoxide at the Jungfraujoch Alpine Station, *Geophys. Res. Lett.*, **21**, 1279–1282, 1994.
- Hanson, D., and K. Mauersberger, Laboratory studies of the nitric acid trihydrate: Implications for the south polar stratosphere, *Geophys. Res. Lett.*, **15**, 855–858, 1988.
- Klein, U., S. Crewell, and R. de Zafra, Correlated millimeter wave measurements of ClO, N₂O and HNO₃ from McMurdo, Antarctica, during polar spring 1994, *J. Geophys. Res.*, **101**, 20,925–20,932, 1996.
- Knox, J. A., On converting potential temperature to altitude in the middle atmosphere, *Eos Trans. AGU*, **79**, 376, 1998.
- Kreher, K., J. G. Keys, P. V. Johnston, U. Platt, and X. Liu, Ground-based measurements of OClO and HCl in austral spring 1993 at Arrival Heights, Antarctica, *Geophys. Res. Lett.*, **23**, 1545–1548, 1996.
- Lee, A. M., H. K. Roscoe, and S. Oltmanns, Model and measurements show Antarctic ozone loss follows edge of polar night, *Geophys. Res. Lett.*, **27**, 3845–3848, 2000.
- Lee, A. M., H. K. Roscoe, A. E. Jones, P. H. Haynes, E. F. Shuckburgh, M. W. Morrey, and H. C. Pumphrey, The impact of the mixing properties within the Antarctic stratospheric vortex on ozone loss in spring, *J. Geophys. Res.*, **106**, 3203–3211, 2001.
- Lee, A. M., R. L. Jones, I. Kilbane-Dawe, and J. A. Pyle, Diagnosing ozone loss in the extratropical lower stratosphere, *J. Geophys. Res.*, **107**(D11), 4110, doi:10.1029/2001JD000538, 2002.
- Lelieveld, J., A. Bregman, H. A. Scheeren, J. Ström, K. S. Carslaw, H. Fischer, P. Siegmund, and F. Arnold, Chlorine activation and ozone destruction in the northern lowermost stratosphere, *J. Geophys. Res.*, **104**, 8201–8213, 1999.
- Li, S., E. C. Cordero, and D. J. Karoly, Transport out of the Antarctic polar vortex from a three-dimensional transport model, *J. Geophys. Res.*, **107**(D11), 4132, doi:10.1029/2001JD000508, 2002.
- Livesey, N. J., W. G. Read, L. Froidevaux, J. W. Waters, M. L. Santee, H. C. Pumphrey, D. L. Wu, Z. Shippony, and R. F. Jarnot, The UARS Microwave Limb Sounder version 5 data set: Theory, characterization, and validation, *J. Geophys. Res.*, **108**(D13), 4378, doi:10.1029/2002JD002273, 2003.
- Manney, G. L., R. W. Zurek, A. O'Neill, and R. Swinbank, On the motion of air through the stratospheric polar vortex, *J. Atmos. Sci.*, **51**, 2973–2994, 1994a.
- Manney, G. L., et al., Chemical depletion of ozone in the Arctic lower stratosphere during winter 1992–93, *Nature*, **370**, 429–434, 1994b.
- Manney, G. L., R. W. Zurek, L. Froidevaux, J. W. Waters, A. O'Neill, and R. Swinbank, Lagrangian transport calculations using UARS data, Part II: Ozone, *J. Atmos. Sci.*, **52**, 3069–3081, 1995.
- Manney, G. L., L. Froidevaux, J. W. Waters, M. L. Santee, W. G. Read, D. A. Flower, R. F. Jarnot, and R. W. Zurek, Arctic ozone depletion observed by UARS MLS during the 1994–95 winter, *Geophys. Res. Lett.*, **23**, 85–88, 1996a.
- Manney, G. L., R. Swinbank, and A. O'Neill, Stratospheric meteorological conditions for the 3–12 Nov 1994 ATMOS/ATLAS-3 measurements, *Geophys. Res. Lett.*, **23**, 2409–2412, 1996b.
- Manney, G. L., L. Froidevaux, M. L. Santee, N. J. Livesey, J. L. Sabutis, and J. W. Waters, Variability of ozone loss during Arctic winter (1991 to

- 2000) estimated from UARS Microwave Limb Sounder measurements, *J. Geophys. Res.*, **108**(D4), 4149, doi:10.1029/2002JD002634, 2003.
- Miller, H. L., R. W. Sanders, and S. Solomon, Observations and interpretation of column OClO seasonal cycles at two polar sites, *J. Geophys. Res.*, **104**, 18,769–18,783, 1999.
- Nagar, V. C., M. K. McDonald, and R. L. de Zafra, Ground-based measurements of stratospheric ClO over Spitzbergen in the Arctic spring of 1997, *J. Geophys. Res.*, **104**, 21,579–21,584, 1999.
- Norton, W. A., and M. P. Chipperfield, Quantification of the transport of chemically activated air from the Northern Hemisphere polar vortex, *J. Geophys. Res.*, **100**, 25,817–25,840, 1995.
- Öllers, M. C., P. F. J. van Velthoven, H. M. Kelder, and L. P. J. Kamp, A study of the leakage of the Antarctic polar vortex in late austral winter and spring using isentropic and 3-D trajectories, *J. Geophys. Res.*, **107**(D17), 4328, doi:10.1029/2001JD001363, 2002.
- Pawson, S., and B. Naujokat, The cold winters of the middle 1990s in the northern lower stratosphere, *J. Geophys. Res.*, **104**, 14,209–14,222, 1999.
- Poole, L. R., and M. C. Pitts, Polar stratospheric cloud climatology based on Stratospheric Aerosol Measurement II observations from 1978 to 1989, *J. Geophys. Res.*, **99**, 13,083–13,089, 1994.
- Raffälski, U., U. Klein, B. Franke, J. Langer, B.-M. Sinnhuber, J. Trentmann, and K. F. Künzi, Ground based millimeter-wave observations of Arctic chlorine activation during winter and spring 1996/97, *Geophys. Res. Lett.*, **25**, 3331–3334, 1998.
- Rex, M., R. J. Salawitch, M. L. Santee, J. W. Waters, K. Hoppel, and R. Bevilacqua, On the unexplained stratospheric ozone losses during cold Arctic Januaries, *Geophys. Res. Lett.*, **30**(1), 1008, doi:10.1029/2002GL016008, 2003.
- Ricaud, P. D., M. P. Chipperfield, J. W. Waters, J. M. Russell III, and A. E. Roche, Temporal evolution of chlorine monoxide in the middle stratosphere, *J. Geophys. Res.*, **105**, 4459–4469, 2000.
- Roscoe, H. K., A. E. Jones, and A. M. Lee, Midwinter start to Antarctic ozone depletion: Evidence from observations and models, *Nature*, **278**, 93–96, 1997.
- Santee, M. L., W. G. Read, J. W. Waters, L. Froidevaux, G. L. Manney, D. A. Flower, R. F. Jarnot, R. S. Harwood, and G. E. Peckham, Inter-hemispheric differences in polar stratospheric HNO₃, H₂O, ClO, and O₃, *Science*, **267**, 849–852, 1995.
- Santee, M. L., G. L. Manney, W. G. Read, L. Froidevaux, and J. W. Waters, Polar vortex conditions during the 1995–96 Arctic winter: MLS ClO and HNO₃, *Geophys. Res. Lett.*, **23**, 3207–3210, 1996a.
- Santee, M. L., et al., Chlorine deactivation in the lower stratospheric polar regions during late winter: Results from UARS, *J. Geophys. Res.*, **101**, 18,835–18,859, 1996b.
- Santee, M. L., G. L. Manney, L. Froidevaux, R. W. Zurek, and J. W. Waters, MLS observations of ClO and HNO₃ in the 1996–97 Arctic polar vortex, *Geophys. Res. Lett.*, **24**, 2713–2716, 1997.
- Santee, M. L., G. L. Manney, N. J. Livesey, and J. W. Waters, UARS Microwave Limb Sounder observations of denitrification and ozone loss in the 2000 Arctic late winter, *Geophys. Res. Lett.*, **27**, 3213–3216, 2000.
- Schiller, C., A. Wahner, U. Platt, H. P. Dorn, J. Callies, and D. H. Ehhalt, Near UV atmospheric absorption measurements of column abundances during Airborne Arctic Stratospheric Expedition, January–February 1989: 2. OClO observations, *Geophys. Res. Lett.*, **17**, 501–504, 1990.
- Schoeberl, M. R., L. R. Lait, P. A. Newman, and J. E. Rosenfield, The structure of the polar vortex, *J. Geophys. Res.*, **97**, 7859–7882, 1992.
- Schoeberl, M. R., R. S. Stolarski, A. R. Douglass, P. A. Newman, L. R. Lait, J. W. Waters, L. Froidevaux, and W. G. Read, MLS ClO observations and Arctic polar vortex temperatures, *Geophys. Res. Lett.*, **20**, 2861–2864, 1993.
- Shindell, D. T., and R. L. de Zafra, Chlorine monoxide in the Antarctic spring vortex: 2. A comparison of measured and modeled diurnal cycling over McMurdo Station, 1993, *J. Geophys. Res.*, **101**, 1475–1487, 1996.
- Shindell, D. T., J. M. Reeves, L. K. Emmons, and R. L. de Zafra, Arctic chlorine monoxide observations during spring 1993 over Thule, Greenland, and implications for ozone depletion, *J. Geophys. Res.*, **99**, 25,697–25,704, 1994.
- Smith, J. B., E. J. Hints, N. T. Allen, R. M. Stimpfle, and J. G. Anderson, Mechanisms for midlatitude ozone loss: Heterogeneous chemistry in the lowermost stratosphere?, *J. Geophys. Res.*, **106**, 1297–1309, 2001.
- Solomon, S., Stratospheric ozone depletion: A review of concepts and history, *Rev. Geophys.*, **37**, 275–316, 1999.
- Solomon, S., S. Borrmann, R. R. Garcia, R. W. Portmann, L. W. Thomason, L. R. Poole, D. Winker, and M. P. McCormick, Heterogeneous chlorine chemistry in the tropopause region, *J. Geophys. Res.*, **102**, 21,411–21,429, 1997.
- Solomon, P., J. Barrett, B. Conner, S. Zoonematkermani, A. Parrish, A. Lee, J. Pyle, and M. Chipperfield, Seasonal observations of chlorine monoxide in the stratosphere over Antarctica during the 1996–1998 ozone holes and comparison with the SLIMCAT three-dimensional model, *J. Geophys. Res.*, **105**, 28,979–29,001, 2000.
- Solomon, P., B. Conner, J. Barrett, T. Mooney, A. Lee, and A. Parrish, Measurements of stratospheric ClO over Antarctica in 1996–2000 and implications for ClO dimer chemistry, *Geophys. Res. Lett.*, **29**(15), 1708, doi:10.1029/2002GL015232, 2002.
- Swinbank, R., and A. O'Neill, A stratosphere-troposphere data assimilation system, *Mon. Weather Rev.*, **122**, 686–702, 1994.
- Toohey, D. W., W. H. Brune, K. R. Chan, and J. G. Anderson, In situ measurements of midlatitude ClO in winter, *Geophys. Res. Lett.*, **18**, 21–24, 1991.
- Toohey, D. W., L. M. Avallone, L. R. Lait, P. A. Newman, M. R. Schoeberl, D. W. Fahey, E. L. Woodbridge, and J. G. Anderson, The seasonal evolution of reactive chlorine in the Northern Hemisphere stratosphere, *Science*, **261**, 1134–1136, 1993.
- Wagner, T., C. Leue, K. Pfeilsticker, and U. Platt, Monitoring of the stratospheric chlorine activation by Global Ozone Monitoring Experiment (GOME) OClO measurements in the austral and boreal winters 1995 through 1999, *J. Geophys. Res.*, **106**, 4971–4986, 2001.
- Wagner, T., F. Wittrock, A. Richter, M. Wenig, J. P. Burrows, and U. Platt, Continuous monitoring of the high and persistent chlorine activation during the Arctic winter 1999/2000 by the GOME instrument on ERS-2, *J. Geophys. Res.*, **107**(D20), 8267, doi:10.1029/2001JD000466, 2002.
- Waters, J. W., Microwave limb sounding, in *Atmospheric Remote Sensing by Microwave Radiometry*, edited by M. A. Janssen, chap. 8, pp. 383–496, John Wiley, New York, 1993.
- Waters, J. W., L. Froidevaux, G. L. Manney, W. G. Read, and L. S. Elson, MLS observations of lower stratospheric ClO and O₃ in the 1992 Southern Hemisphere winter, *Geophys. Res. Lett.*, **20**, 1219–1222, 1993a.
- Waters, J. W., L. Froidevaux, W. G. Read, G. L. Manney, L. S. Elson, D. A. Flower, R. F. Jarnot, and R. S. Harwood, Stratospheric ClO and ozone from the Microwave Limb Sounder on the Upper Atmosphere Research Satellite, *Nature*, **362**, 597–602, 1993b.
- Waters, J. W., G. L. Manney, W. G. Read, L. Froidevaux, D. A. Flower, and R. F. Jarnot, UARS MLS observations of lower stratospheric ClO in the 1992–1993 and 1993–1994 Arctic winter vortices, *Geophys. Res. Lett.*, **22**, 823–826, 1995.
- Waters, J. W., et al., Validation of the UARS Microwave Limb Sounder ClO measurements, *J. Geophys. Res.*, **101**, 10,091–10,127, 1996.
- Waters, J. W., et al., The UARS and EOS Microwave Limb Sounder (MLS) experiments, *J. Atmos. Sci.*, **56**, 194–218, 1999.
- Waugh, D. W., and W. J. Randel, Climatology of Arctic and Antarctic polar vortices using elliptical diagnostics, *J. Atmos. Sci.*, **56**, 1594–1613, 1999.
- Waugh, D. W., W. J. Randel, S. Pawson, P. A. Newman, and E. R. Nash, Persistence of the lower stratospheric polar vortices, *J. Geophys. Res.*, **104**, 27,191–27,201, 1999.
- Wehr, T., S. Crewell, K. Künzi, J. Langen, H. Nett, J. Urban, and P. Hartogh, Remote sensing of ClO and HCl over northern Scandinavia in winter 1992 with an airborne submillimeter radiometer, *J. Geophys. Res.*, **100**, 20,957–20,968, 1995.
- World Meteorological Organization, Scientific assessment of ozone depletion: 1998, *Global Ozone Res. Monit. Proj. Rep. 44*, Geneva, 1999.
- World Meteorological Organization, Scientific assessment of ozone depletion: 2002, *Global Ozone Res. Monit. Proj. Rep. 47*, Geneva, 2003.
- Zurek, R. W., G. L. Manney, A. J. Miller, M. E. Gelman, and R. M. Nagatani, Interannual variability of the north polar vortex in the lower stratosphere during the UARS mission, *Geophys. Res. Lett.*, **23**, 289–292, 1996.

N. J. Livesey, M. L. Santee, and J. W. Waters, Jet Propulsion Laboratory, Mail Stop 183-701, 4800 Oak Grove Drive, Pasadena, CA 91109, USA. (livesey@mmls.jpl.nasa.gov; mls@mmls.jpl.nasa.gov; joe@mmls.jpl.nasa.gov)
G. L. Manney, Department of Natural Sciences, New Mexico Highlands University, Las Vegas, NM 87701, USA. (manney@mmls.jpl.nasa.gov)